NORTHWESTERN UNIVERSITY
CHEMISTRY DEPARTMENT
EVANSTON, IL 60208

DEVELOPMENT OF HIGHLY-CONDUCTIVE POLYELECTROLYTES FOR LITHIUM BATTERIES

NASA GRANT NAG3-2628
June 1, 2001 – November 30, 2002

FINAL TECHNICAL REPORT
PREPARED FOR
NASA-LEWIS RESEARCH CENTER
CLEVELAND, OH 44135

by

D.F. SHRIVER, PI
M. A. RATNER, Co-PI
S. VAYNMAN, Co-PI
K.O. ANNAN, Post-Doctoral Fellow
J.F. SNYDER, Graduate Student

March 4, 2003

INTRODUCTION

Future NASA and Air Force missions require reliable and safe sources of energy with high specific energy and energy density that can provide thousands of charge-discharge cycles at more than 40% depth-of-discharge and that can operate at low temperatures.

All solid-state batteries have substantial advantages with respect to stability, energy density, storage life and cyclability. Among all solid-state batteries, those with flexible polymer electrolytes offer substantial advantages in cell dimensionality and commensurability, low temperature operation and thin film design. The above considerations suggest that lithium-polymer electrolyte systems are promising for high energy density batteries and should be the systems of choice for NASA and US Air Force applications.

Polyelectrolytes (single ion conductors) are among most promising avenues for achieving a major breakthrough in the applicability of polymer-based electrolyte systems. Their major advantages include unit transference number for the cation, reduced cell polarization, minimal salt precipitation, and favorable electrolyte stability at interfaces. Our research is focused on synthesis, modeling and cell testing of single ion carriers, polyelectrolytes.

During the first year of this project we attempted the synthesis of two polyelectrolytes. The synthesis of the first one, the poly(ethyleneoxide methoxy acrylate-co-lithium 1,1,2-trifluorobutanesulfonate acrylate, was attempted few times and it was unsuccessful. We followed the synthetic route described by Cowie and Spence[1]. The yield was extremely low and the final product could not be separated from the impurities. The synthesis of this polyelectrolyte is not described in this report.

The second polyelectrolyte, comb polysiloxane polyelectrolyte containing oligoether and perfluoroether sidechains, was synthesized in sufficient quantity to study the range of properties such as thermal stability, Li-ion-conductivity and stability toward lithium metal. Also, the batteries containing this polyelectrolyte were assembled and tested. The results are detailed below.

The synthesis of another polyelectrolyte similar to polysiloxane polyelectrolyte has been started, however, the synthesis was not completed due to termination of the project.

SYNTHESIS OF POLYSILOXANE POLYELECTROLYTE CONTAINING OLIGOETHER AND PERFLUOROETHER SIDECHAINS

To achieve high ionic conductivity in polyelectrolytes it is important to promote local anion mobility within polyelectrolyte systems. The most direct method for accomplishing local anion motion is to place them at the terminal end of flexible sidechains. The flexible sidechains provide increased motion to the anions independent of the segmental motion of the polymer backbone, thereby enhancing the cation conductivity. The basicity of the anion influences the degree of ion pairing that occurs in

the system, which may inhibit high conductivity. A flexible and high-dielectric polymer host promotes long-range cation diffusion, whereas crystalline ion-polymer systems result in low cation conductivities. In addition, a significant number of accessible polar groups must be present to provide cation coordination sites within the polymer matrix. The synthesis of the polyelectrolyte presented below addresses all of these factors to optimize the conductivity of comb polyelectrolyte.

Polysiloxanes provide a good polymer host for highly conductive comb polyelectrolytes. These materials consist of a highly flexible $[Si\text{-}O]_n$ backbone, which may have glass transition temperatures as low as -100 °C.

The ion conductivities of several types of polysiloxane polymer-salt complexes, such as linear copolymers of poly(dimethyl siloxane) and poly(ethylene oxide) have demonstrated room temperature conductivities in 10^{-4} to 10^{-5} S/cm range when complexed with lithium salts.[2,3,4] Similar conductivities were demonstrated by for comb polymer-salt complexes consisting of lithium perchlorate and poly(methylsiloxane) with poly(ethylene oxide) sidechains.[5-8] Ion conductivity in comb polyelectrolytes such as polysiloxanes with lithium alkylsulfonate-terminating oligoether sidechains was reported to be ~10^{-6} S/cm.[9-11] The decrease in conductivity in comparison to polymer-salt complexes is due in part to the elimination of conductive anions. Although additional studies have also been performed on these materials there has been little development of polysiloxane polyelectrolytes with high lithium ion conductivity. Such systems are interesting for electrochemical applications due to the high power density of lithium.

The studies presented here seek to decrease ion pairing in comb polysiloxane polyelectrolytes through development of weakly basic anions. The electron-withdrawing nature of fluorine is often used to decrease the basicity of anions in polymer electrolytes. The cation conductivity has been shown to increase considerably for a polyether/salt hybrid polymer electrolyte using alkylsulfonamide anions when the neighboring alkyl group is fluorinated. This increase has been attributed to the change in dissociation constant, since there was negligible change in the other system parameters including T_g and polymer molecular weight. The trifluoromethansulfonate anion (abbreviated "triflate") has been known since the 1950s to favor ion dissociation[12] and it does not have the explosion hazards of the perchlorate anion. However, the high mobility of the triflate anion in polymer-salt complexes often results in low cation transference numbers. The incorporation of larger, completely fluorinated alkyl chains with terminal lithium sulfonate groups has demonstrated encouraging ionic conductivities of ~10^{-6} S/cm in blends with PEO.[13-15]

The synthesis of functionalized polysiloxanes can be accomplished by two general methods. The first entails polymerization of a functionalized precursor. Polymerization may be accomplished by hydrolysis of the appropriate chlorosilane, and condensation of the resultant siloxanol, as shown in Scheme 1.[16]

$$R_2SiCl_2 + 2H_2O \longrightarrow R_2Si(OH)_2 + 2HCl$$

$$nR_2Si(OH)_2 \longrightarrow H[OR_2Si]_mOH + [OSiR_2]_{cyclic} + (n\text{-}1)H_2O$$

Scheme 1. One of the possible routes for the synthesis of functionalized polysiloxanes

However, this approach has significant problem; synthesis results in low molecular weight polymer. The condensation reaction in Scheme1 is an equilibrium process that often results in a small number of polymer-repeat units and a wide distribution of molecular weights.[17] The ring-opening polymerization of an appropriately functionalized cyclic polysiloxane offers better control over the reaction conditions. However, this also is an equilibrium reaction that often results in low molecular weight polymers that display poor mechanical properties.[18]

A second method for synthesizing comb polysiloxanes is to functionalize a pre-made polymer, such as poly(methylhydrosiloxane), PMHS. Such polymers are useful because they are commercially available and they tend to have acceptable numbers of repeat units. Although polymers such as PMHS are restricted to only one sidechain per repeat unit, the relatively high molecular weight of the resultant functionalized polymer electrolyte often imparts better mechanical properties than those that are synthesized by polymerization reactions shown in Scheme 1. We used the second method to synthesize polyelectrolyte as described below.

The most common technique to functionalize poly(hydro)siloxanes is a platinum-catalyzed hydrosilylation reaction.[19] This reaction involves the addition of a carbon-carbon double bond to a hydrosilane unit. Hydrosilylation reactions take place under relatively mild conditions and can accommodate a wide range of unsaturated compounds.[20] Speier's catalyst, chloroplatinic acid,[21] and Karstedt's catalyst, Pt(0) tetramethyldivinyldisiloxane,[22-25] are two the most often used catalysts. Karstedt's catalyst is preferred due to its higher activity and lower incidence of side reactions.[26,27]

Scheme 2, which details the hydrosilylation reaction, emphasizes the importance of platinum colloid formation prior to the catalytic cycle. The formation of platinum colloids is indicated by a yellow solution color and it has been found to be dependent on the presence of oxygen.[28] Oxygen has also been shown to deter irreversible platinum colloid agglomeration.[29] Colloid agglomeration is known to significantly reduce the activity of the catalyst[30] and is most readily detected by a shift in solution color to dark brown or black. In addition, oxygen may predispose the Pt/SiH complex to nucleophilic attack by an olefin. The influence of electron-withdrawing groups adjacent to the olefin tends to hinder the reaction rate.[31] In contrast, the incidence of electron-withdrawing groups attached to the siloxane backbone tends to encourage it.

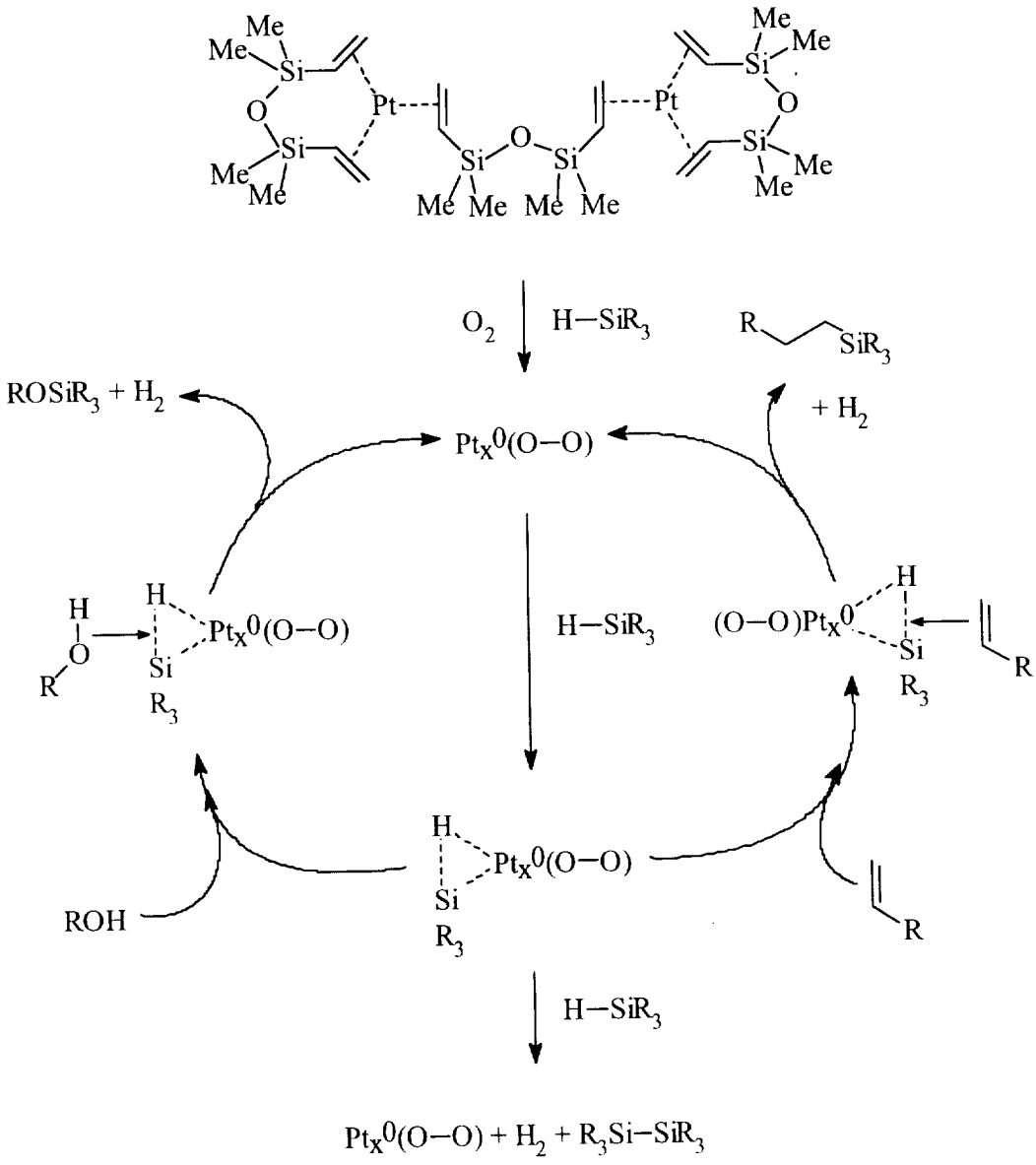

Scheme 2. A route for the synthesis of functionalized polysiloxanes that is used in the present work

Several comb polyelectrolytes, depicted in Figure 1, were synthesized using a procedure described in detail in the Appendix. Changes in the lithium to etheric oxygen ratio (Li:EO) were achieved by altering the relative concentration of the perfluoroether and oligoether sidechains. The ratios of the oligoether sidechains to the perfluoroether sidechains were high enough to assure a favorable dielectric constant for the polymer matrix. The oligoether length was chosen to achieve an amorphous phase through the range of investigated temperatures.

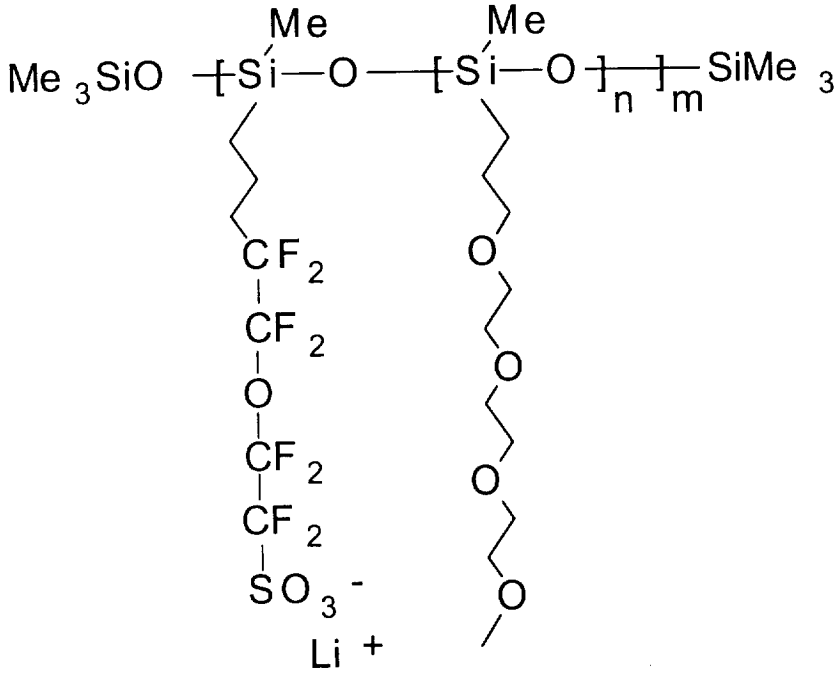

Figure 1. An optimized polyelectrolyte

GLASS TRANSITION TEMPERATURE

Differential scanning calorimetry (DSC) data were collected on ca. 5 mg samples of thoroughly dried polyelectrolytes using a Perkin-Elmer Pyris 1 differential scanning calorimeter fitted with a liquid nitrogen cooling apparatus. The temperature was varied between –110 and 140°C at 6 heating rates from 5 to 40 °C/min, and the reported T_g values were obtained by extrapolating the halfway point of the transition curves to zero heating rate. Figure 2 shows that at any Li:EO ratio the glass transition temperature is lower than 260°K.

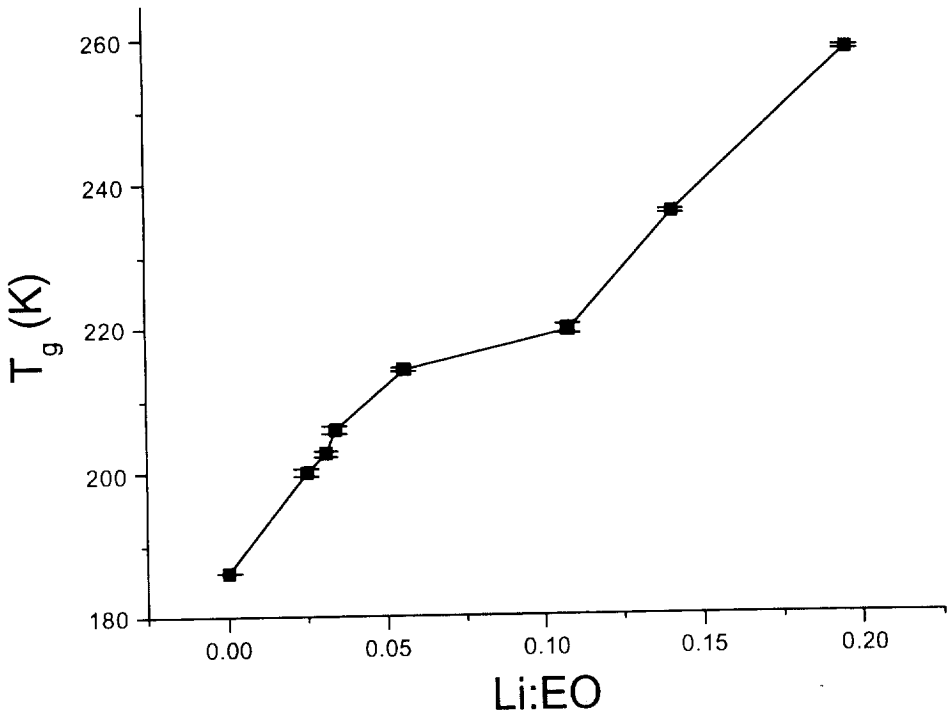

Figure 2. The change in T_g with Li:EO ratio

As evident from Figure 2, at low concentrations of lithium ions, T_g increases in a rapid linear fashion as the Li:EO ratio is increased. This effect is attributed to coordination between an ion and different segments of the polymer chain, which binds those segments together. A similar result is found for covalent crosslinking agents.

An interesting anomaly exists in the region between 0.05 Li:EO and 0.10 Li:EO where T_g increases only slightly. This anomaly is not likely to be the result of measurement error for several reasons. The thermal response of each sample was measured in at least six consecutive heat-cool cycles of varying rate. The data plotted in Figure 2 result from linear extrapolation to zero heating rate and have very small average deviations, generally about 0.1K, even smaller than indicated by the error bars. All of the samples within the anomalous region were measured on the same day. In addition, a second aliquot of some of the samples was remeasured as a check. The T_g were highly repeatable. A similar anomaly was observed for analogous polymer-salt complexes.[32] It is hypothesized that the perfluoroalkyl sidechains depress the T_g and effectively act as internal plasticizers.[33-34] Ionic crosslinking predominates at low ion and perfluoroalkyl sidechain concentrations. At higher ion concentrations the T_g is depressed by ~10 K from the values expected by extrapolation of the low ion concentration data.

The polyelectrolytes corresponding to Li:EO ratios higher than 0.05 are rubbery and posses no noticeable fluidity at room temperature. Li:EO ratios at or lower than 0.03 resulted in poor mechanical properties, although this may be improved by crosslinking.[35]

IONIC CONDUCTIVITY

Complex impedance spectra were obtained over a frequency range of 5 KHz to 13 MHz using a Hewlett Packard HP4192A impedance analyzer, and over a frequency range of 10 Hz to 60 KHz using a Solartron 1286 electrochemical interface with a Solartron 1250 Frequency Response Analyzer. There was no discernable difference between the spectra obtained from either analyzer for a given sample in a comparable frequency range. The sample was contained in a hollow Teflon disk of known dimensions, and sandwiched between two stainless-steel blocking electrodes in an airtight cell. All manipulations were carried out in a dry box under nitrogen atmosphere. A typical sample was 2.90 mm thick and 5.15 mm in diameter. Measurements were performed over a temperature range of 258-383 K in a Sun Oven environmental chamber where the temperature was regulated with an air bath (± 0.1 °C). Cole-Cole plots of the spectra were fit to a parallel resistor-constant phase element (C.P.E.) equivalent circuit with a non-linear least squares routine to determine the bulk resistance. The DC conductivity was calculated from the measured resistance using the Nernst-Einstein equation. Plots of conductivity versus 1/T were fit to the VTF equation with a non-linear least squares fit routine.

Figure 3 displays an impedance plot for a polyelectrolyte with EO:Li = 41. A semi-circle was fit to the data using a non-linear least-squares program. Broadening is evident in the semi-circle along the real axis at low temperatures. In these cases, the semi-circle function was fit to the more reliable high frequency data.

Impedance measurements were performed at different temperatures and than the data were then plotted on Arrhenius coordinates as shown in Figure 4. The curvatures in the figure suggest that ion transport is coupled to polymer motion in accord with the Williams-Landel-Ferry (WLF) description of conductivity.[36-39] The T_g for each sample is sufficiently low to suggest that a completely amorphous matrix exists within the temperature range studied. In a non-crystalline matrix the properties of the sample may be described by the following empirical Vogel-Tamman-Fulcher (VTF)[40-42] equation:[43]

$$\sigma T = \sigma_0 e^{\frac{B}{k(T-T_0)}}$$

The data for each sample was therefore fit to the VTF equation using a non-linear least-squares program.

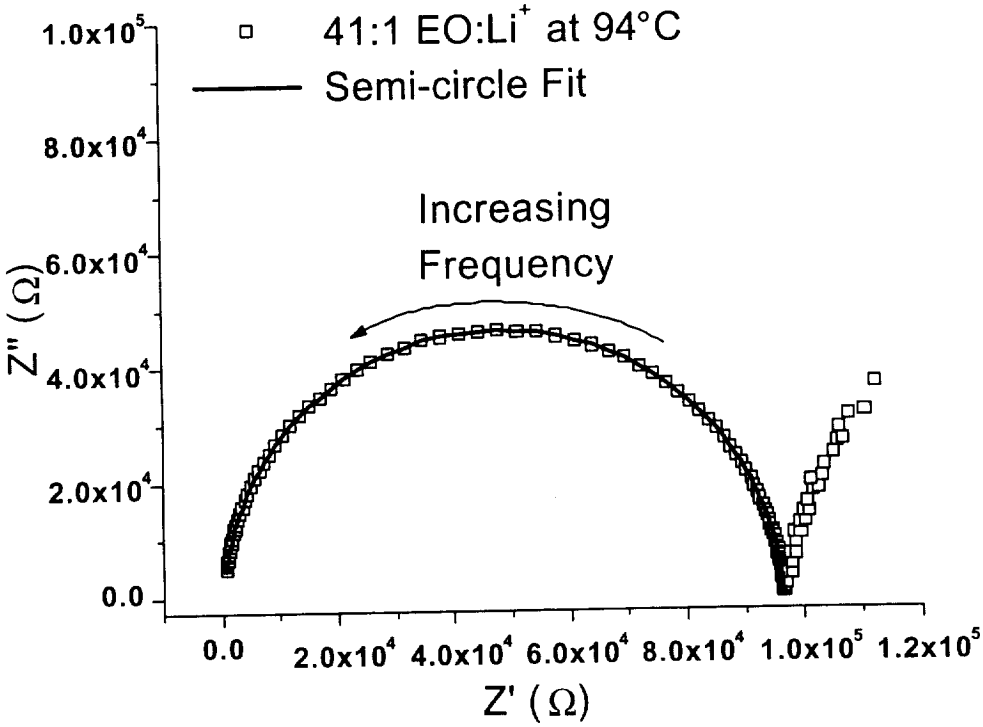

Figure 3. The typical impedance plot. Polyelectrolyte with 41:1 EO:Li ratio at 94°C

Figure 5 illustrates the conductivity changes at two temperatures as the ratio of the perfluoroether sidechains to the oligoether sidechains increases. The increase in temperature brings about an increase in conductivity by about an order of magnitude, as well as a shift in the conductivity peak toward higher lithium ion concentrations. The existence of a maximum in this curve has been noted elsewhere.[1,44,45] The initial rise in conductivity may be attributed to the increase in the number of charge carriers. The decrease in conductivity at higher ion concentrations is often attributed to ion aggregation and ionic crosslinking, which slow ion mobility, decrease the effective number of charge carriers, and increase T_g.

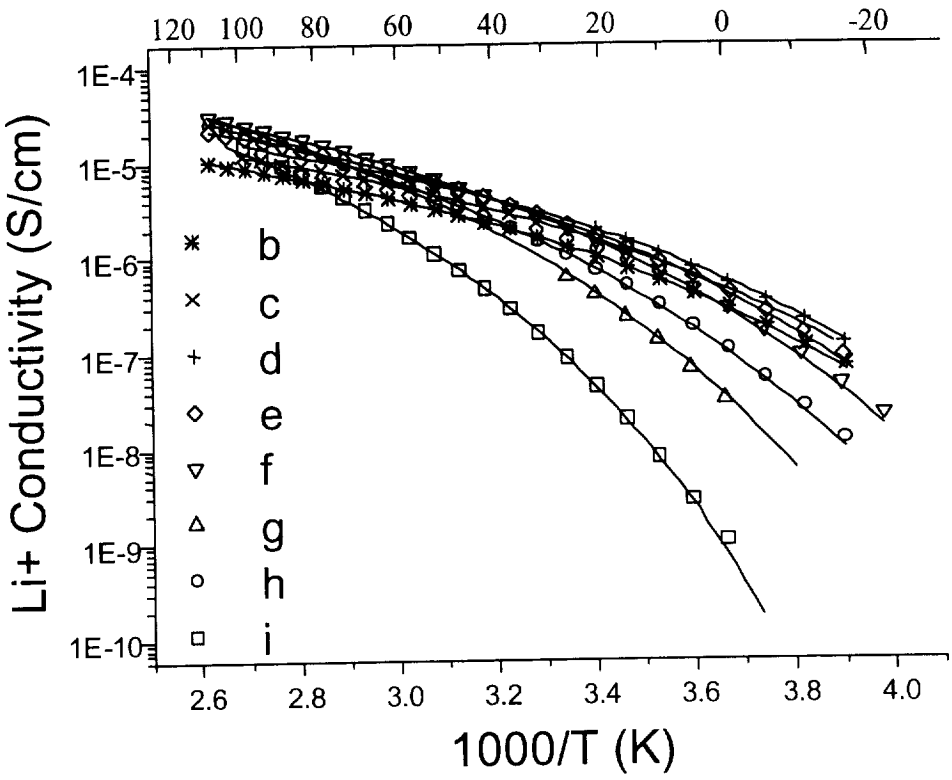

Figure 4. Arrhenius curves for polyelectrolyte with different Li:EO ratio: b - 0.019; C – 0.024; d – 0.030; e – 0.034; f – 0.056; g – 0.110; h – 0.140; i – 0.200

Thus, highly conductive comb polyelectrolytes have been synthesized that consist of a polysiloxane backbone with oligoether and lithium-sulfonate terminating perfluoroether sidechains.

The polyelectrolyte with 33:1 EO to Li ratio that has the highest conductivity was selected for further research. A new, bigger batch of this polyelectrolyte was synthesized. It's chemical purity, ionic conductivity and glass transition temperature were determined. These properties were similar to the batch described previously.

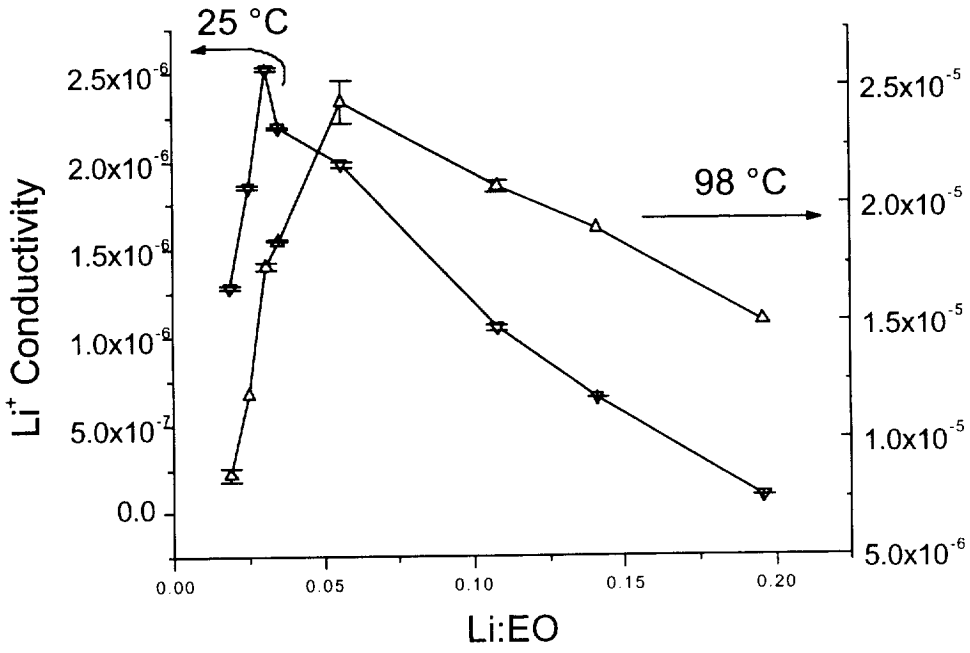

Figure 5. Conductivity of polyelectrolyte as a function of the EO:Li ratio and temperature

REACTIVITY OF POLYELECTROLYTE TOWARD LITHIUM METAL

To be used in the batteries polyelectrolyte is supposed to have good resistance toward lithium metal. This was investigated by measuring impedance of the symmetrical Li/polyelectrolyte/Li cell. Results of this investigation are shown in Figures 6 and 7.

It is evident that resistance of the cell increases steadily with time thus indicating instability of polyelectrolyte in contact with the metal. A highly resistant interface between metal and polyelectrolyte is formed. The reactivity of this polyelectrolyte with lithium precludes its use in the lithium battery. However, lithium/polyelectrolyte cell was assembled to determine the capacity of such cell.

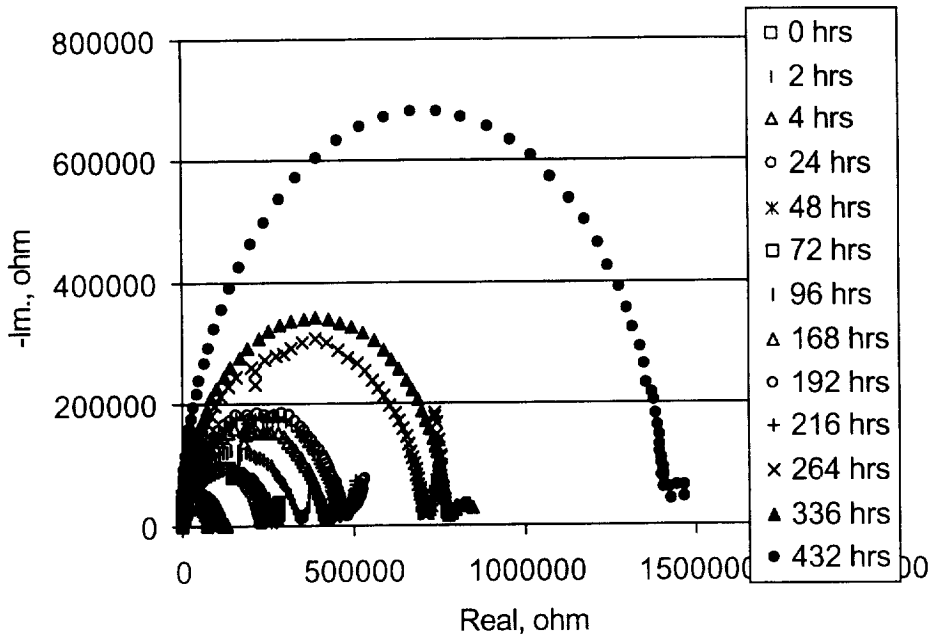

Figure 6. Impedance of the Li/polyelectrolyte/Li cell at 25°C

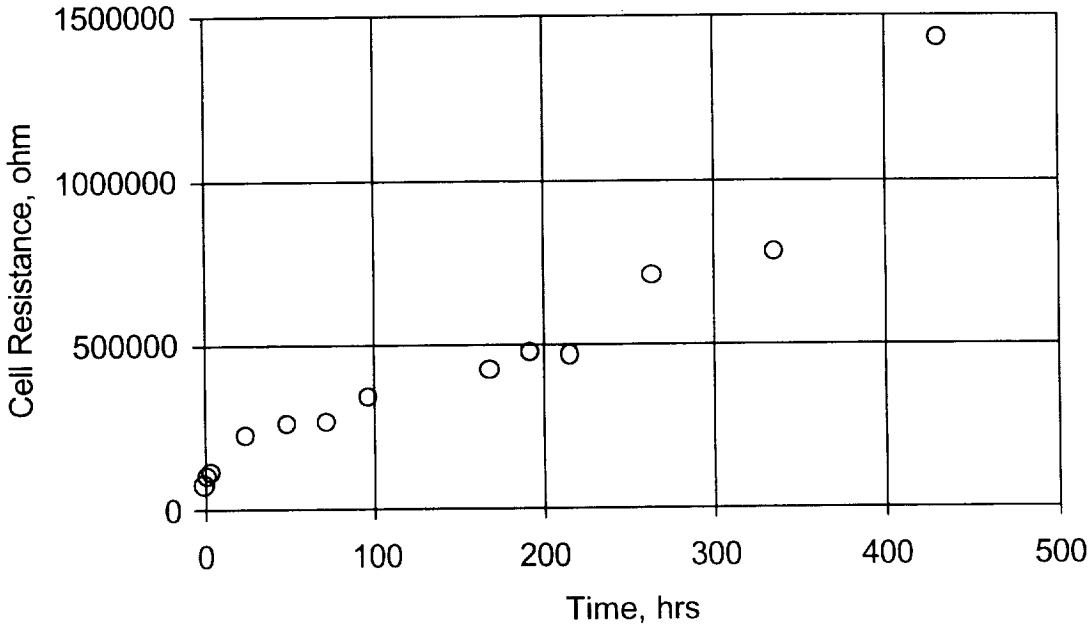

Figure 7. Resistance of the Li/polyelectrolyte cell at 25°C

PERFORMANCE OF THE POLYELECTROLYTE IN THE BATTERY

The construction of battery components and assembly of cells was performed in a glove box under argon. Cylindrical cells were used (Figure 8). Lithium foil (0.015-inch thick and 0.375-inch in diameter) was used as an anode. The 3 V cathode material, Li_xMnO_2 (80%), carbon (10%) and polyelectrolyte (10%) was spread over another stainless steel current collector which served as the cathode. The anode, electrolyte, and cathode were pressed together in the cylindrical cell. The cells were cycled at room temperature at 0.015 mA/cm^2 charge/discharge current.

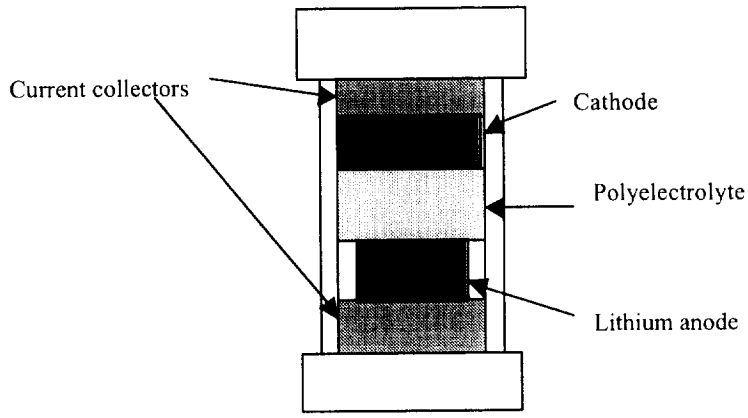

Figure 8. Cell assembly (not to scale)

Performance of the cell is depicted in Figure 9. While the cell capacity in the first discharge is approximately 80 mAh/cm^2 per gram of active cathode material, it drops significantly in the next few cycles indicating the formation of the highly resistive interface between lithium and polyelectrolyte.

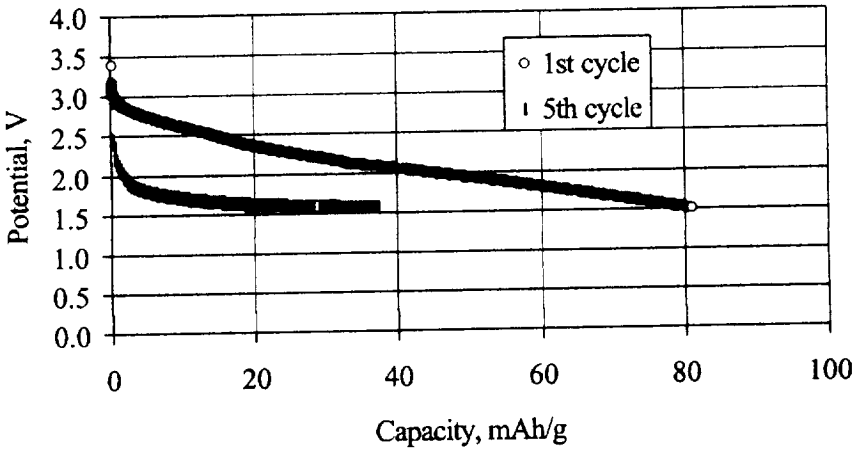

Figure 9. Discharge of Li/polyelectrolyte cell at 0.015mA/cm^2 at 25°C

APPENDIX. DETAILS OF SYNTHESIS OF COMB POLYSILOXANE POLYELECTROLYTES CONTAINING OLIGOETHER AND PERFLUOROETHER SIDECHAINS

Materials. Tetrafluoro-2-(tetrafluoro-2-iodoethoxy)ethane-sulfonyl fluoride (**1**) was provided by Professor Shisheng Zhu and it was stored over activated 4Å molecular sieves. All other reagents were purchased from the Aldrich Chemical Co. and, unless otherwise noted, were used without further purification. Since **1** is light sensitive and extremely moisture-sensitive it was shielded from bright light and handled under dry nitrogen. Synthesis of the intermediate compounds is described below (Scheme A.1-A.3).

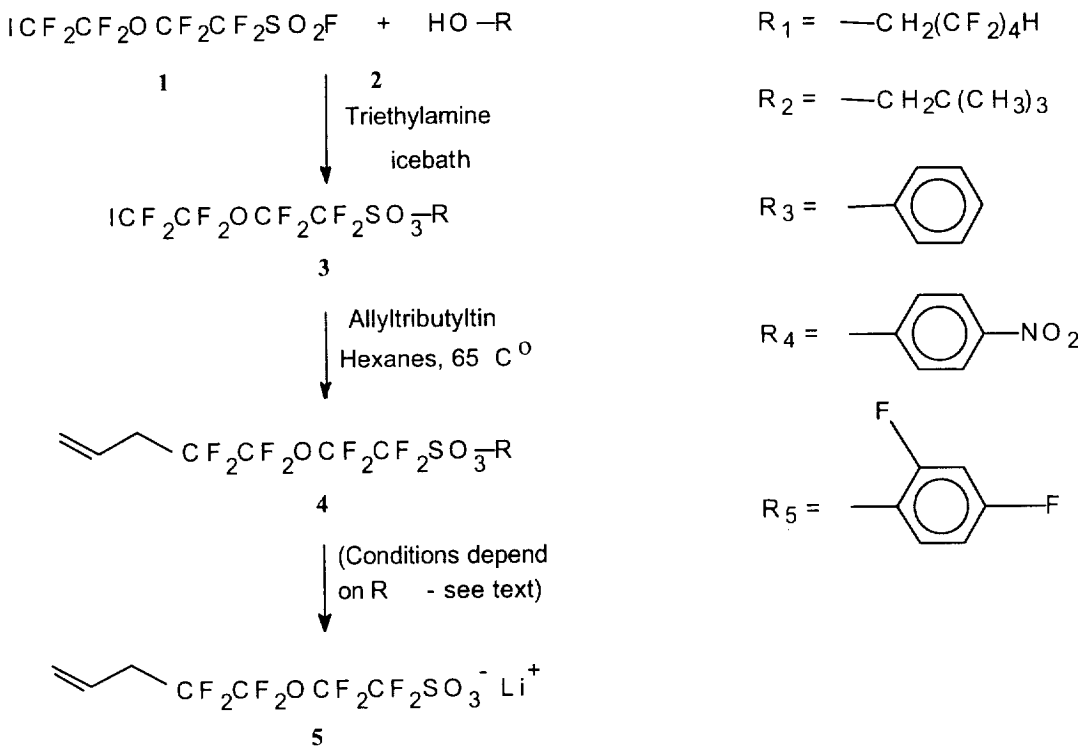

Scheme A.1.

Preparation of Alkyl and Phenyl alkanesulfonates (3)

$ICF_2CF_2OCF_2CF_2S(O)_2O$-R

In an N_2-purged glovebox, 0.1 mol of the alcohol reagent (**2**, previously dried over activated 4 Å molecular sieves) and 40 mL triethylamine (distilled from CaH_2) were added to a flask fitted with a pressure-equalizing addition funnel. When the highly

deactivated alcohol 4-nitrophenol was used the proton transfer rate was slow. The reaction is facilitated by a high dielectric solvent, so a mixture of 25 mL triethylamine and 45 mL acetonitrile (distilled from CaH_2) was employed. The reaction solution was chilled in an ice bath, and 0.05 mol of **1** was added dropwise with stirring. The distribution of products was found to be very sensitive to the reaction conditions. Fast addition of **1** or early removal of the ice bath resulted in a loss of up to 40% of the reagents to sideproducts, so the flask was allowed to warm to room temperature only after it was maintained in the ice bath for eight hours. Under these optimized conditions, less than 2% of the reagents were lost to sideproducts. After 24-48 hours of stirring at room temperature a dark solution resulted and the ^{19}F NMR peak at δ45 (sulfonyl fluoride) was no longer present. The reaction mixture was then quenched in 100 mL of deionized water, producing two liquid phases. 1M HCl was slowly added to the two-phase system until the aqueous phase became acidic. The organic phase was extracted with 3x75 mL of hexane. The hexane fractions were combined and washed with 2x100 mL deionized H_2O, followed by 3x100 mL portions of 10% KOH solution in deionized H_2O. The hexane solution was washed with 4x100 mL deionized H_2O, until the aqueous fraction was neutral. The organic phase was dried with $MgSO_4$, filtered, and hexane evaporated at 40°C. Further purification was achieved by fractional distillation under vacuum. About 5% loss in yield occurred during purification.

2,2,3,3,4,4,5,5-Octafluoropentyl tetrafluoro-2-(tetrafluoro-2-iodoethoxy)ethanesulfonate (3 / R_1) was prepared according to the general procedure for **3** in high yield based on **1**, as determined *in-situ* by ^{19}F NMR spectroscopy: density 1.96 g/mL; ^1H NMR δ 6.03 (triplet of triplets, 1, J = 52 Hz, 5 Hz), 4.82 (t, 2, J = 12 Hz). ^{19}F NMR δ -65.97 (t, 2, J = 6 Hz), -82.79 (t, 2, J = 13 Hz), -85.91 (septet, 2, J = 6 Hz), -114.34 (s, 2), -120.63 (quintet, 2, J = 11 Hz), -125.35 (s, 2), -130.01 (m, 2), and -137.69 (doublet of quintets, 2, J = 52 Hz, 3 Hz).

Neopentyl tetrafluoro-2-(tetrafluoro-2-iodoethoxy)ethanesulfonate (3 / R_2) was prepared according to the general procedure for **3** in high yield based on **1**, as determined *in-situ* by ^{19}F NMR spectroscopy: ^1H NMR δ 4.14 (s, 2), 0.95 (m, 9). ^{19}F NMR δ -65.70 (m, 2), -82.86 (m, 2), -85.89 (m, 2), and –115.13 (m, 2).

Phenyl tetrafluoro-2-(tetrafluoro-2-iodoethoxy)ethanesulfonate (3 / R_3) was prepared according to the general procedure for **3** in high yield based on **1**, as determined *in-situ* by ^{19}F NMR spectroscopy: bp 72°C (0.05 Torr); ^1H NMR δ 7.45 (m, 5); ^{19}F NMR δ -65.39 (s, 2), -82.17 (t, 2, J = 19 Hz), -85.71 (s, 2), and –113.26 (s, 2).

4-Nitrophenyl tetrafluoro-2-(tetrafluoro-2-iodoethoxy)ethanesulfonate (3 / R_4) was prepared according to the general procedure for **3** in high yield based on **1**, as determined *in-situ* by ^{19}F NMR spectroscopy. The crude ester, a dark orange solid, decomposes rapidly at elevated temperatures. Purification was accomplished by crystallizing the with hexanes to yield a light yellow powder: IR (neat) 1535 and 1349 cm^{-1} (NO_2) and 603 cm^{-1} (C-I). ^1H NMR δ 8.37 (d, 2, J = 9 Hz), 7.49 (d, 2, J = 9 Hz). ^{19}F NMR δ -65. (t, 2, J = 6 Hz), -81 (t, 2, J = 12 Hz), -85. (sept, 2, J = 6 Hz), and -112 (s, 2).

2,4-Difluorophenyl tetrafluoro-2-(tetrafluoro-2-iodoethoxy)ethanesulfonate (3 / R_5) was prepared according to the general procedure for **3** in high yield based on **1**, as determined *in-situ* by ^{19}F NMR spectroscopy: density 1.63 g/mL; ^{1}H NMR δ 7.34 (triplet of doublets, 1, J = 9 Hz, 5 Hz), 7.01 (triplet of doublets, J = 9 Hz, 3 Hz), 6.94 (triplet of triplets, J = 8 Hz, 2 Hz); ^{19}F NMR δ -65.87 (t, 2, J = 6 Hz), -82.34 (t, 2, J = 12 Hz), -85.92 (septet, 2, J = 6 Hz), -108.08 (quintet, 1, J = 7 Hz), -113.61 (s, 2), -121.95 (sextet, 1, J = 7 Hz).

Preparation of Alkyl and Phenyl 4-(Prop-1-ene)-tetrafluoro-2-(tetrafluoro-2-ethoxy)ethanesulfonates (4)

$CH_2CHCH_2CF_2CF_2OCF_2CF_2S(O)_2O$-R

0.0015 mol of AIBN and 60mL of hexane were transferred to a flame-dried Schlenk flask, which was then immersed in an ice bath and dry N_2 was bubbled through the mixture for 30 minutes. To this solution 0.02 mol allyltributyltin (purged with N_2) and 0.01 mol **3** were added by syringe under a N_2 atmosphere. The flask was partially evacuated, sealed, and transferred to an oil bath at 65°C. The solution was stirred for 8 hrs and then allowed to cool to room temperature. Completion of the reaction was indicated by a shift in the ^{19}F NMR peak from δ-66 (I-CF_2-) to δ-118 (Allyl-CF_2-).

The hexanes were removed by rotary evaporation at 50°C. The product was then added to a concentrated aqueous solution of 0.015 mol potassium fluoride dihydrate in a Teflon container and thoroughly agitated to convert $ISnBu_3$ to $FSnBu_3$. The resulting white precipitate formed an emulsion, which was broken up with 20 mL acetone, filtered, and washed with acetone, which was removed from the filtrate under vacuum at 40°C. 75 mL diethyl ether was then added and potassium fluoride was extracted with 3x100 mL of deionized water. The organic fraction was dried over $MgSO_4$ and filtered. Ether was then removed from the filtrate under vacuum at 40°C, resulting in two immiscible phases. ^{1}H and ^{19}F NMR indicate the presence of both allyltributyltin and **4** in each phase. The two components were separated and purified using dry flash chromatography.[46] The separation was monitored with ^{1}H and ^{19}F NMR, and thin-layer chromatography. Allyltributyltin has an R_f = 0.72 in hexanes on silica. The silica column was eluted in 75 mL fractions with hexanes until allyltributyltin was removed. The elutent was then changed to 10 vol% ether in hexanes. The product-containing fractions were combined, dried over $MgSO_4$, filtered, and the solvent was removed at 50°C under vacuum. The resulting clear, colorless liquid was stored under N_2 over activated 4Å molecular sieves. About 15% loss in yield occurred during purification.

2,2,3,3,4,4,5,5-Octafluoropentyl 4-(prop-1-ene)-tetrafluoro-2-(tetrafluoro-2-ethoxy)ethanesulfonate (4 / R_1) was prepared according to the general procedure for **4** in high yield based on **3**, as determined *in-situ* by ^{19}F NMR spectroscopy: ^{1}H NMR δ 6.04 (triplet of triplets, 1, J = 52 Hz, 5 Hz), 5.78 (m, 1), 5.33 (d, 1, J = 9 Hz), 5.32 (d, 1, J = 19 Hz), 4.82 (t, 2, J = 12 Hz), 2.81 (triplet of doublets, 2, J = 18 Hz, 7 Hz). ^{19}F NMR δ -82.71 (t, 2, J = 13 Hz), -87.72 (septet, 2, J = 6 Hz), -114.40 (s, 2), -117.61 (s, 2), -120.54

(quintet, 2, J = 11 Hz), -125.24 (s, 2), -129.90 (m, 2), and -137.56 (doublet of quintets, 2, J = 52 Hz, 3 Hz).

Neopentyl 4-(prop-1-ene)-tetrafluoro-2-(tetrafluoro-2-ethoxy)ethanesulfonate (4 / R_2) was prepared according to the general procedure for **4** in high yield based on **3**, as determined *in-situ* by ^{19}F NMR spectroscopy: ^{1}H NMR δ 5.69 (m, 1), 5.21 (m, 2), 2.81 (m, 2). ^{19}F NMR δ -83.15 (m, 2), -88.44 (m, 2), -117.92 (m, 2), and –118.42 (m, 2).

Phenyl 4-(prop-1-ene)-tetrafluoro-2-(tetrafluoro-2-ethoxy)ethanesulfonate (4 / R_3) was prepared according to the general procedure for **4** in high yield based on **3**, as determined *in-situ* by ^{19}F NMR spectroscopy: R_f = 0.15 (hexanes on silica); ^{1}H NMR δ 7.45 (m, 5), 5.77 (m, 1), 5.30 (m, 2), 2.80 (triplet of doublets, 2, J = 18 Hz, 8 Hz); ^{19}F NMR δ -82.40 (t, 2, J = 13 Hz), -87.83 (t, 2, J = 13 Hz), –113.59 (s, 2), and –117.66 (t, 2, J = 18 Hz).

4-Nitrophenyl 4-(prop-1-ene)-tetrafluoro-2-(tetrafluoro-2-ethoxy)ethanesulfonate (4 / R_4) was prepared according to the general procedure for **4** in high yield based on **3**, as determined *in-situ* by ^{19}F NMR spectroscopy: ^{1}H NMR δ 8.35 (d, 2, J = 9 Hz), 7.49 (d, 2, J = 9 Hz), 5.77 (m, 1), 5.33 (d, 1, J = 8 Hz), 5.32 (d, 1, J = 18 Hz), 2.82 (triplet of doublets, 2, J = 18 Hz, 7 Hz); ^{19}F NMR δ -82.38 (t, 2, J = 12 Hz), -87.68 (t, 2, J = 12 Hz), -113.00 (s, 2), and –117.54 (t, 2, J = 18 Hz).

2,4-Difluorophenyl 4-(prop-1-ene)-tetrafluoro-2-(tetrafluoro-2-ethoxy)ethanesulfonate (4 / R_5) was prepared according to the general procedure for **4** in high yield based on **3**, as determined *in-situ* by ^{19}F NMR spectroscopy: density 1.48 g/mL; ^{1}H NMR δ 7.34 (triplet of doublets, 1, J = 9 Hz, 5 Hz), 7.01 (triplet of doublets, J = 9 Hz, 3 Hz), 6.94 (triplet of triplets, J = 8 Hz, 2 Hz), 5.77 (m, 1), 5.31 (d, 1, J = 10 Hz), 5.30 (d, 1, J = 17 Hz), 2.82 (triplet of doublets, 2, J = 18 Hz, 7 Hz); ^{19}F NMR δ -82.36 (t, 2, J = 12 Hz), -87.81 (t, 2, J = 13 Hz), -108.15 (quintet, 1, J = 7 Hz), -113.76 (t, 2, J = 3 Hz), -117.57 (t, 2, J = 18 Hz), -122.03 (sextet, 1, J = 7 Hz).

Preparation of 4-(Prop-1-ene)-tetrafluoro-2-(tetrafluoro-2-ethoxy)ethanesulfonic acid, lithium salt (5)

$CH_2CHCH_2CF_2CF_2OCF_2CF_2S(O)_2O^-$ Li^+

In a 100 mL flask fitted with a condenser, 8 mmol of **4** was added to 40 mmol LiOH and 50 mL THF. The mixture was refluxed overnight and then cooled to room temperature. Much of the excess LiOH was removed from the resulting slurry by filtration. THF was removed on a rotary evaporator and replaced by 40 mL pentane to form a light yellow precipitate, which was filtered off. Pentane was removed on a rotary evaporator and replaced by 40 mL hexane to precipitate the product. Minor losses in yield occurred during purification. Table A.1 lists the success of reaction for several protecting groups. When the lithium salt of the sulfonate group was prepared, up to 100% of the phenol byproduct was also converted to the lithium salt, as indicated by ^{1}H and ^{19}F NMR spectroscopy. ^{1}H NMR δ 5.78 (m, 1), 5.33 (d, 1, J = 9 Hz), 5.32 (d, 1, J =

19 Hz), 2.80 (triplet of doublets, 2, J = 18 Hz, 7 Hz); ^{19}F NMR δ -83.2 (s, 2), -88.5 (s, 2), -117.8 (s, 2), -118.1 (s, 2).

3-(Methoxytriethoxy)-prop-1-ene (6) $CH_2CHCH_2(OCH_2CH_2)_3OCH_3$

Dropwise addition of 100 mL of tri(ethyleneglycol)monomethylether (103 g, 0.625 mole, previously dried over activated 4Å molecular sieves) to a magnetically stirred slurry of 24.6 g NaH (1.03 mole) in 150 mL tetrahydrofuran (THF, freshly distilled from Na-benzophenone) under dry N_2 resulted in evolution of H_2 and formation of $NaO(CH_2CH_2O)_3CH_3$. After gas evolution ceased the flask was cooled to 0°C and 80 mL of allylchloride (75 g, .98 mol) was added dropwise. The flask was allowed to warm to room temperature, stirred overnight, and then chilled in an ice bath. Dropwise addition of 80 mL of 2-propanol in dry THF (1:1) eliminated the excess NaH. The solution was allowed to warm to room temperature and stirred for 2 hours. The resulting slurry was filtered three times through Celite to remove precipitated NaCl. It was then concentrated on a rotary evaporator, resulting in a thick yellow liquid that was purified by distillation under reduced pressure. ^{1}H NMR δ 5.90 (m, 1), 5.20 (multiplet of quartets, 2), 3.96 (doublet of quartets, 2), 3.57 (m, br, 10), 3.47 (m, 2), 3.33 (s, 3).

Co-functionalization of poly(methyl(hydro)siloxane) with 3-(Methoxytriethoxy)-prop-1-ene and 2,2,3,3,4,4,5,5-Octafluoropentyl 4-(prop-1-ene)-tetrafluoro-2-(tetrafluoro-2-ethoxy)ethanesulfonate (8)

Precisely weighed (*c.a.* 1.0 g, 0.016 mole) amounts of poly(methylhydrosiloxane) (7, n = ~35.1; previously dried over activated 4Å molecular sieves) were transferred under a flow of dry N_2 into purged, flame-dried Schlenk flasks along with 20 mL dry toluene and 30 μL Karstedt's catalyst. The desired amount of **4** /$\mathbf{R_1}$ (dried over activated 4Å molecular sieves) was precisely weighed and added by syringe. Dry air was bubbled through the solution for fifteen minutes to introduce a catalytic amount of oxygen. The reaction mixture was then sealed and heated to 80°C with stirring until the reaction was complete (ca. 30 hours). The extent of sidechain attachment was determined by ^{19}F NMR, and completion of the reaction was verified by loss of the ^{1}H NMR allyl peaks at δ 5.78, δ 5.33, and δ 5.32.

A quantity of **6** was then added in up to 15% molar excess of the calculated remaining methylhydrosiloxane repeat units. The solution was bubbled with dry N_2 for 30 minutes, partially evacuated, resealed, and heated to 80°C for 48 hours with magnetic stirring. Toluene was then removed on a rotary evaporator at 70°C. Nearly complete functionalization of the polymer was determined by the significant reduction of the FT-IR band at 2161cm^{-1}, and loss of the ^{1}H NMR peak at δ4.7. Residual silane content in the purified product was determined to be no greater than 3% in all cases by ^{1}H NMR end-group analysis. Residual platinum content in most samples was determined to be no greater than 10% of the content of lithium ions by weight, and to have no significant effect on the impedance of the samples. When a greater quantity of platinum was added, samples were filtered through a dry flash column consisting of 11 g activated carbon sandwiched between two layers of 4 g Celite. The column was washed with 2 x 40 mL toluene before applying the sample in a solution of 20 mL toluene, and it was eluted with

toluene. This process was monitored by ^{1}H and ^{19}F NMR. Fractions were collected and volatiles were removed under vacuum at 70°C, to produce a clear golden product.

$[OSi(CH_3)(CH_2CH_2CH_2CF_2CF_2OCF_2CF_2SO_3CH_2CF_2CF_2CF_2CF_2H)\ (OSi(CH_3)H)_x]_n$ ^{1}H NMR δ 6.11 (t, 1, J = 56 Hz), 4.85 (s, 2), 4.64 (s, br, n*x), 2.00 (m, br, 2), 1.57 (m, br, 2), 0.55 (m, br, 2), 0.06 (m, br, 3); ^{19}F NMR δ -82.46 (m, br, 2), -87.90 (m, br, 2), -114.16 (m, br, 2), -118.51 (m, br, 2), -120.20 (m, br, 2), -124.94 (m, br, 2), -129.50 (m, br, 2), -137.27 (m, br, 2).

$[OSi(CH_3)(CH_2CH_2CH_2(OCH_2CH_2)_3OCH_3)]_{n*x}$ ^{1}H NMR δ 3.64 (m, br, 12), 3.36 (m, br, 5), 1.57 (m, br, 2), 0.46 (m, br, 2), 0.03 (m, br, 3).

Deprotection of the sulfonate group to form the lithium salt. (9)

In a N_2-purged glovebox, anhydrous lithium bromide beads were weighed to milligram precision in a 1:1 molar ratio to the perfluoroether sidechain on the polymer. The beads were dissolved in 20 mL of 2-butanone and added to the polymer. The reaction flask was partially evacuated and then stirred for 48 hours at 75°C. The extent of deprotection was determined by ^{19}F NMR. Solvent and low-molecular weight byproducts were removed at 80°C under vacuum. $BrCH_2(CF_2)_4H$ and residual 3-(methoxytriethoxy)-prop-1-ene were removed by repeated extraction with hexane. A high yield of the lithium salt was determined by ^{19}F NMR *in-situ*, but some loss of product occurred during extraction. $[OSi(CH_3)(CH_2CH_2CH_2CF_2CF_2OCF_2CF_2SO_3^- Li^+)\ (OSi(CH_3)H)_x]_n$ ^{1}H NMR δ 4.80 (s, br, n*x), 2.21 (m, br, 2), 1.64 (m, br, 2), 0.71 (m, br, 2), 0.20 (m, br, 3); ^{19}F NMR δ -83.99 (m, br, 2), -89.74 (m, br, 2), -119.27 (m, br, 2), -119.40 (m, br, 2). $[OSi(CH_3)(CH_2CH_2CH_2(OCH_2CH_2)_3OCH_3)]_{n*x}$ ^{1}H NMR δ 3.60 (m, br, 10), 3.50 (m, br, 3), 3.45 (m, br, 2), 3.31 (m, br, 2), 1.66 (m, br, 2), 0.61 (m, br, 2), 0.17 (m, br, 3).

Several comb polyelectrolytes, depicted in Figure 1 (previous section), were synthesized from polymethylhydrosiloxane by hydrosilylation reactions. Changes in the etheric oxygen to lithium ratio (EO:Li) were accomplished by altering the relative concentration of the perfluoroether and oligoether sidechains. The large number of electron-withdrawing fluorine groups in proximity to the terminal sulfonate group should reduce the anion basicity. The ether linkage within the perfluorinated sidechain may help to introduce flexibility and increase the dielectric constant. The ratios of the oligoether sidechains to the perfluoroether sidechains are high enough to assure a favorable dielectric constant for the polymer matrix. The oligoether length was chosen to achieve an amorphous phase through the range of investigated temperatures. Similar polymer-salt complexes based on PMHS display crystallization at temperatures as high as –7°C when the poly(ethylene oxide) sidechains include 7 etheric oxygens.

The target oligoether sidechain and perfluorosulfonate sidechain were synthesized with terminal allyl groups to facilitate hydrosilylation of the sidechains to the polysiloxane backbone. Attempts to react vinyl-terminated perfluoroalkyl molecules with PMHS resulted in poor yields.

3-(Methoxytriethoxy)-prop-1-ene was prepared in a one-pot synthesis from tri(ethyleneglycol)monomethylether by reacting an alkoxide of the reagent with allyl chloride.[47] Similar reactions for tetrafluoro-2-(tetrafluoro-2-iodoethoxy)ethane-sulfonyl fluoride, **1**, using allyl alcohol have yields reported to be as low as 50%.[48-49] A simpler method for introducing allyl functionality to the perfluoroether compound involves an AIBN-initiated radical reaction with allyltributyltin,[50,51] which proceeded quickly in the presence of terminal chloride and iodide groups. Conversion of the tributyltin iodide byproduct to tributyltin fluoride, which is insoluble in most solvents, facilitated purification.[52] Excess allyltributyltin, residual tributyltin iodide, and other impurities were removed using dry flash chromatography.[46]

Tetrafluoro-2-(tetrafluoro-2-iodoethoxy)ethanesulfonyl fluoride, **1**, was the precursor for the perfluoroether sidechain. The multi-step alteration of **1** to the perfluoroether sidechain is detailed in Scheme 1. The sulfonyl fluoride group was converted to a sulfonate ester to avoid reaction of the sulfonyl halide with moisture. The sulfonate ester protecting group allowed the formation of the lithium salt under a range of conditions.

The addition of an alcohol-functionalized compound to sulfonyl fluoride provides a convenient route to form a sulfonate ester.[53-55] This reaction involves a proton-transfer facilitated by triethylamine.[56] Triethylamine serves the additional function of absorbing the caustic byproduct, hydrogen fluoride, as it is generated. Each molecule of triethylamine may form a complex with up to 3 molecules of HF.[57] This complexation of HF helps to prevent erosion of the glass reaction flask and it simplifies the purification of the product, **3**, as shown in Scheme A.2.

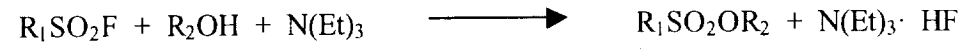

Scheme A.2.

In comparison to pure triethylamine, the complex between triethylamine and HF has low solubility in nonpolar solvents, and favorable solubility in polar solvents. A similar effect is seen with 1:1 complexes involving triethylamine and hydrochloric acid. The addition of excess HCl to the quenched reaction ensures that all of the triethylamine reacted with either HF or HCl. This facilitated separation of triethylamine from **3**. Several combinations of solvents for this separation are cited in the literature, of which the most common pair is water and diethyl ether.[58-60] In the present investigation, extraction with hexanes from water provided an efficient high yield purification of **3**.

The use of a high-dielectric co-solvent such as acetonitrile increased the rate of proton transfer for the reaction described in Scheme A.2.[61-63] The reaction is usually exothermic, and so the reaction vessel was contained in an ice bath to minimize byproduct formation at higher temperatures. Thoroughly dry reagents were used to prevent hydrolysis of the sulfonyl fluoride.

A convenient approach for deprotecting a perfluorosulfonate group to yield the lithium salt involves the use of LiBr in 2-butanone. This reaction has been shown to be effective with 2,2-dimethyl propane, $\mathbf{R_2}$[64,65] As indicated in Table A.1, LiBr was not effective in displacing aryl protecting groups. When $\mathbf{R_2}$ was used as the protecting agent the deprotection and purification during the final step were difficult to verify *in-situ* by standard techniques. In contrast, the protecting group $\mathbf{R_1}$ resulted in a product yield of 100% as well as a simple and quantifiable means of monitoring the protecting group using ^{19}F NMR analysis. For these reasons $\mathbf{R_1}$ was used as the protecting group for all of the polyelectrolytes discussed in this work.

Table A.1.[i] Percent yield data resulting from preparation of the lithium salt from several perfluoroalkylsulfonate esters

	LiBr[ii]	**LiOH**[iii]
4-methoxyphenyl triflate[iv]	3%[v]	2%
1-napthyl triflate[iv]	0%	94%
4 / $\mathbf{R_1}$	100%	
4 / $\mathbf{R_2}$	100%	
4 / $\mathbf{R_3}$		0%
4 / $\mathbf{R_4}$	0%	100%
4 / $\mathbf{R_5}$	0%	100%

i. Yields are based on the formation of the desired product as determined by ^{19}F NMR. For the sake of accurate comparison, possible reductions in overall yield due to purification were not taken into account. ***4 / R_x*** *refers to the compound* ***4*** *in Scheme 1 with the corresponding protecting group, $R_1 - R_5$.*

ii. The appropriate sulfonate reagent was added to a solution of up to 6 equivalents of LiBr in 2-benzophenone and allowed to reflux for 48 hours.

iii. The appropriate sulfonate reagent was added to a solution of 6 equivalents of LiOH in THF and allowed to reflux for 48 hours.

iv. These commercially available compounds were used to approximate ***4*** *with 4-methoxyphenyl or 1-napthyl protecting groups.*

v. No reaction after 48 hours. 3% free triflate was detected after 5 days of reflux.

Two additional methods were explored for preparing the lithium salt of the aryl-protected sulfonate group. The first alternate approach involved an adaptation of the Stille palladium-catalyzed coupling reaction using organotriflates.[66-68] Although the Stille reaction is fundamentally a coupling reaction, the lithium salt of a perfluorosulfonate group is often a byproduct.[66] Stille reported high yields of the coupling reaction for triflates of substituted phenyl groups.[67] Yields greater than 50% were not obtained in the present research for protecting groups listed in Table A.1.

In the second method for preparing the lithium salt of the aryl-protected sulfonate group an excess of LiOH in THF was employed. Nucleophilic attack by hydroxide results in formation of the initial alcohol used in Scheme A.1. The reaction was found to be complementary to reactions involving LiBr, as shown in Table A.1. Due to the susceptibility of siloxane bonds to nucleophilic attack, this method was employed prior to attaching the sidechains to the polymer. The purified lithium salt of the sidechain, **5**, was obtained, but it was found to be only partially soluble in the solvents required for the hydrosilylation reaction. Attempts to perform the hydrosilylation in high yields with the lithium salt were unsuccessful.

The sidechains **4** (with protecting group $\mathbf{R_1}$) and **7** were synthesized and purified, and then covalently bound to polymethylhydrosiloxane by the hydrosilylation reaction as shown in Scheme 3. The manufacturer of PMHS confirmed that the method of production results in a polymer consisting of only methylhydro-siloxane repeat units, so no dimethylsiloxane or dihydrosiloxane repeat units should be present.[69] MALDI MS experiments were performed with the PMHS precursor and an a-cyano-4-hydroxycinnamic acid matrix. A strong peak at ~1524 daltons and minor repeat peaks every 60 daltons indicated an average backbone repeat unit number of $n \sim 23$. ^{1}H NMR end-group analysis of an aliquot of PMHS purified through repeated fractional precipitations with hexanes from methanol[70,71] confirmed an average backbone repeat unit number between 20 and 25. ^{1}H NMR end-group analysis of the final product also suggested a similar number of repeat units. Based on this value for n, the sizes of the final polyelectrolytes were calculated to be in the 6000-8000 dalton range.

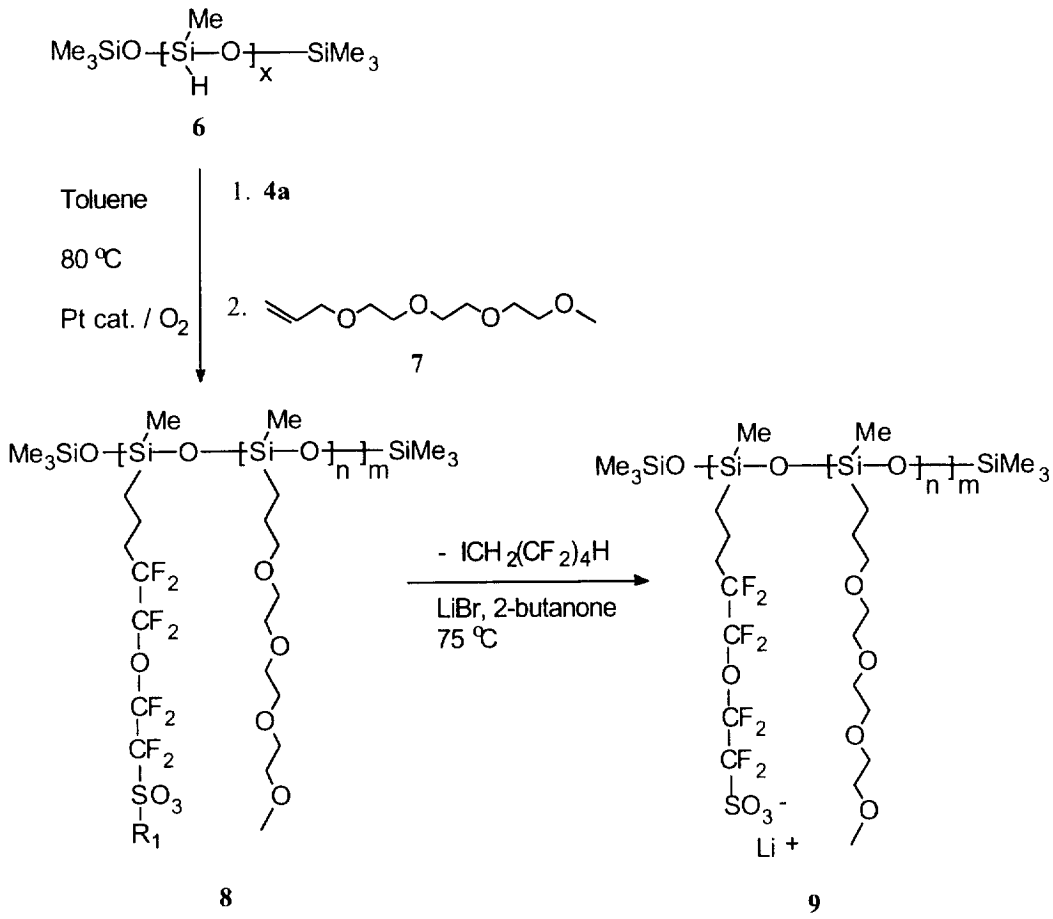

Scheme A.3.

The reaction between PMHS and the allyl-functionalized perfluoroether was promoted by dry air and it went to completion within 24 hours, as determined by ^{19}F NMR. Oxygen predisposes the Pt/SiH complex to nucleophilic attack,[72] and thereby counteracts the influence of electron-withdrawing fluorine groups adjacent to the olefin.[73] Oxygen also facilitates the formation of platinum colloids,[72] which are essential in the catalytic cycle proposed by Lewis.[74,75] Furthermore, oxygen deters undesirable platinum colloid agglomeration.[76,77] The formation of platinum colloids is indicated by a yellow solution color whereas the presence of platinum colloid aggregates shifts the solution color to dark brown or black. Platinum colloid aggregates were removed by filtering the final product through activated carbon.

A 40-hour reaction period provided 97% sidechain hydrosilylation of the polymer, as determined by ^{1}NMR end-group analysis. Complete functionalization of PMHS was never attained, even under conditions of high temperatures, excess reagents, or long reaction times. The incomplete functionalization was indicated by the presence

of a silane peak at 2160cm^{-1} in the infrared spectrum. The slow reaction rate of the last few silane groups is attributed primarily to steric factors.

Deprotection reactions with lithium bromide proceeded with little difficulty. High purity anhydrous lithium bromide beads were added in increments until the total amount equaled the number of moles of perfluoroether sidechain. The result of each addition was monitored by ^{19}F NMR, and the percent yield determined *in-situ* corresponded to the calculated percent yield within the expected margin of error (typically 1 mg). Since minor losses of polymer were anticipated in samples that were filtered through activated carbon, an estimate was made of the total quantity of lithium bromide to be added. This estimate was refined by the use of ^{19}F NMR peak integrations following each incremental addition.

^{13}C, ^{1}H, and ^{19}F NMR spectra were obtained on a Varian 400 MHz spectrometer. For most samples, $CDCl_3$ was used as the solvent and TMS was the internal reference for ^{1}H NMR. $CFCl_3$ was the external reference for ^{19}F NMR. Polysiloxane samples were analyzed in $CDCl_3$ and residual $CHCl_3$ was used as the internal reference.[78] Polyelectrolytes with high lithium ion concentrations (<30 EO:Li) were found to be insoluble in chloroform, so these samples were analyzed in deuterated acetone.

Infrared spectra were acquired on a Bio-Rad FTS-60 spectrometer on neat samples prepared in an inert atmosphere glovebox and contained between KBr or CaF_2 plates. FT-IR spectra were used to check the dryness of polysiloxane polyelectrolytes. Raman spectra were acquired on a Bio-Rad FT-Raman spectrometer on samples under N_2 in sealed capillary tubes.

^{13}C and ^{1}H NMR spectra of the compounds synthesized in the present work agree with those reported in the literature for similar compounds. ^{1}H NMR end-group analysis was used to determine the distribution ratio of the oligoether and perfluoroether sidechains, as well as the residual silane content. The theoretical sidechain distribution ratio was calculated from the amount of the starting materials, which often had a lower EO:Li ratio than expected. Some loss of product occurred during purification. The ^{1}H NMR spectra for **9d** (33 EO:Li; c.f. Table 2) in Figure A.2 contain peaks that are clearly resolved. Accurate and repeatable integration values were obtained by expanding the region of interest, as shown in the inset spectrum. Peak values are listed in the experimental section. Comparison of peak H_a (δ2.2) to peaks H_b and H_c (apparent as one singlet, δ1.6) were used to determine the ratio of the oligoether and perfluoroether sidechains. Calculations of the EO:Li ratio were also performed using NMR integrations of the other peaks. In each case the EO:Li ratio was found to be very close to the estimated ratio.

Table A.2. Li:EO ratio for synthesized polyelectrolytes (Table includes T_g data also)

	Li:EO	EO:Li	T_g (K)
9a	0.00	∞	186
9b	0.019	54	200
9c	0.024	41	200
9d	0.030	33	203
9e	0.034	29	206
9f	0.056	18	214
9g	0.11	9.3	220
9h	0.14	7.1	236
9i	0.20	5.1	258

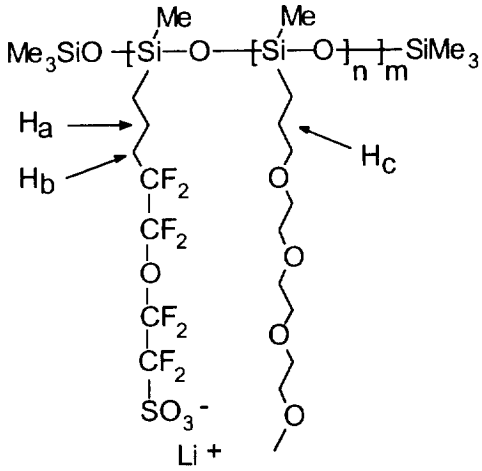

Figure A.2. ^{1}H NMR spectrum of a typical polyelectrolyte in $CDCl_3$. The EO:Li =33.

Residual silane protons on the polymer appear at δ4.8, and they are present in less than 3% of the total number of sidechains. The peak at δ0.2 is composed of both the siloxymethyl repeat units (3**n* H / polymer, where *n* is the number of repeat units) and the terminal trimethylsiloxane peaks (18 H / polymer). Comparison of the integrated peak with the integrations of the other peaks indicates ~24 repeat units, which is very close to the average *n* of 23 obtained by MALDI MS reported above.

^{19}F NMR solution spectroscopy was used to determine progress of the reaction and percent yield. ^{19}F NMR also was used to determine removal of the protecting groups in the deprotection reaction.

FT-IR spectra were used to determine the residual silane groups (by the stretch at 2160 cm^{-1}) in the final polyelectrolytes, and residual water when the polyelectrolytes were dried. As shown in Figure 3a, the CF_2 (asymmetric stretch 1350-1200 cm^{-1}, symmetric stretch 1200-1080 cm^{-1}), Si-R (890-690 cm^{-1}), and Si-O-Si (1080, 1020 cm^{-1},

broad) stretching modes dominate the region between 1500 cm^{-1} and 500 cm^{-1}. These bands make it difficult to detect lithium complexation of SO_3 groups and lithium complexation of PEO, as detected by C-O-C stretching and bending modes within this region. The FT-Raman spectra, such as Figure 3b, did not contain a peak at 867 cm^{-1} associated with an $M\text{-}O_n$ symmetric stretch "breathing mode" found in high molecular weight PEO complexes[79] and macrocyclic complexes[80] with alkali metal salts. The absence of this band may be due to the short oligoether sidechain lengths, or more probably to the lowered symmetry expected around the lithium ions in the polyelectrolyte.

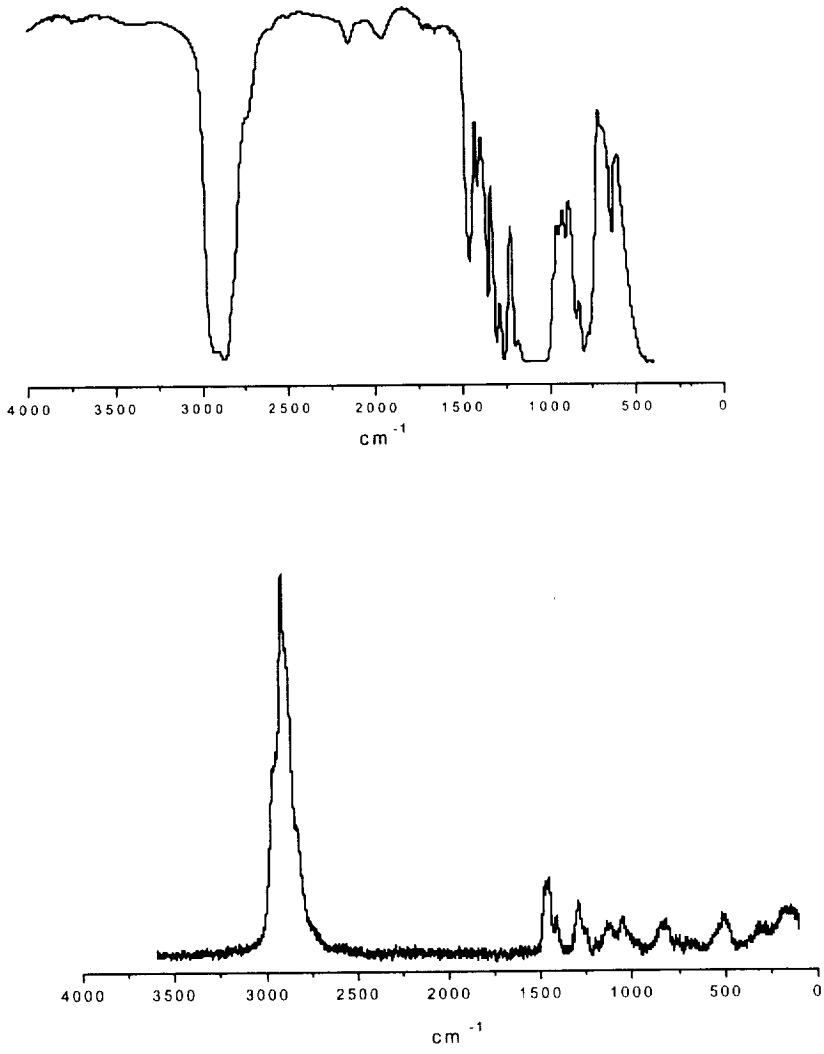

Figure A.3. (a) FT-IR and (b) FT-Raman spectra of the polyelectrolyte depicted in Figure A.2.

REFERENCES

1. J. G. Cowie, and G. H. Spence, *Solid State Ionics*, **123**, 233 (1999)
2. Nagaoka, K.; Naruse, H.; Shinohara, D.; Watanabe, M. *J. Polym. Sci. Polym. Lett. Ed.*, **22**, 659 (1984).
3. Adamic, K. J.; Greenbaum, S. G.; Wintersgill, M.; Fontanella, J. J. *J. Appl. Phys.*, **60**, 1342 (1986).
4. Albinsson, I.; Jacobsson, P.; Mellander, B.-E.; Stevens, J. R. *Solid State Ionics*, **53-56**, 1044 (1992).
5. Fish, D.; Khan, I. M.; Smid, J. *Polym. Prepr. (Am. Chem. Soc., Div. Polym. Chem.*, **27**, 325 (1986).
6. (26) Fish, D.; Khan, I. M.; Smid, J. *Makromol. Chem., Rapid Commun.*, **7**, 115 (1986).
7. Fish, D.; Khan, I. M.; Wu, E.; Smid, J. *Br. Polym. J.*, **20**, 281 (1988).
8. Khan, I. M.; Yan, Y.; Fish, D.; Wu, E.; Smid, J. *Macromolecules*, **21**, 2684 (1988).
9. Zhou, G. B.; Khan, I. M.; Smid, J. *Polym. Prepr. (Am. Chem. Soc., Div. Polym. Chem.)*, **30**, 416 (1989).
10. Zhou, G. B.; Khan, I. M.; Smid, J. *Polym. Commun.*, **30**, 52 (1989).
11. Zhou, G. B.; Khan, I. M.; Smid, J. *Macromolecules*, **26**, 2202 (1993).
12. Haszeldine, R. N.; Kidd, J. M. *J. Org. Chem.*, 4228 (1954).
13. Gorecki, W.; Donoso, P.; Berthier, C.; Mali, M.; Roos, J.; Brinkmann, D.; Armand, M. B. *Solid State Ionics*, **28-30**, 1018 (1988).
14. Ullrich, S. A.; Gard, G. L.; Nafshun, R. L.; Lerner, M. M. *J. Fluorine Chem.*, **79**, 33 (1996).
15. Hamaide, T.; Le Deore, C. *Polymer*, **34**, 1038 (1993).
16. Chojnowski, J. In *Siloxane Polymers*, Clarson, S. J., Semlyen, J. A., Eds.; PTR Prentice Hall: Englewood Cliffs, NJ, 1993; p. 1.
17. Saam, J. C. In Silicon Base Polymer Science, Zeigler, J. M., Fearon, F. S., Eds.; American Chemical Society: Washington DC, 1990; p. 71
18. Hutchison, J. C. Studies of Ion Mobility in Polyelectrolytes Based on Aluminosilicate Polymer Composites and Polysiloxanes, PhD Thesis, Northwestern University, 1998, p. 71.
19. Speier, J. L.; Webster, J. A. Barnes, G. H. *J. Am. Chem. Soc.*, **79**, 974 (1957).
20. Ojima, I. In *The chemistry of Organic Silicon Compounds*, Patai, S., Rappoport,, Z., Eds.; John Wiley & Sons, Ltd., 1989; p. 1480
21. Speier, J. L.; Webster, J. A. Barnes, G. H. *J. Am. Chem. Soc.*, **79**, 974 (1957).
22. Karsedt, B. D. U.S. Patent 3,775,452, 1973.
23. Karsedt, B. D. *Chem. Abstr.*, **80**, 16134j (1974).
24. Chandra, G.; Lo, P.Y.; Hitchcock, P. B.; Lappert, M. F. *Organometallics*, **6**, 191 (1987).
25. Lewis, L. N.; Colborn, R. E.; Grade, H.; Bryant, Jr., G. L.; Sumpter, C. A.; Scott, R. A. *Organometallics*, **14**, 2202 (1995).
26. Lestel, L.; Cheradam, H.; Boileau, S.; *Polymer*, **31**, 1154 (1990).
27. Mehl, G.; Goodby, J. W. *Angew. Chem. Int. Ed. Engl.*, **35**, 2641 (1996).
28. (18) Lewis, L. N.; Lewis, N. *Chem. Mater.*, **1**, 106 (1989).

29. Speier, J. L. *Adv. Organomet. Chem.*, **17**, 407 (1979).
30. Lewis, L. N. *Chem.Rev.*, **93**, 2693 (1993).
31. Lewis, L. N.; *J. Am. Chem. Soc.*, **112**, 5998 (1990).
32. J. F. Snyder, *Ion and Polymer Mobility in Flexible Comb Polymer Electrolytes*, p.168, PhD Thesis, Northwestern University, (2002).
33. M. Kono, E. Hayashi, M. Watanabe, *J. Electrochem. Soc.*, **145**, 1521 (1998).
34. S. W. Hu, Z. C. Zhang, F. Yi, S. B. Fang, X. F. Zhang, and F. M. Li, *Chinese J. Polym. Sci.*, **18**, 109 (2000).
35. J. M. G. Cowie, and K. Sadaghianizadeh, *Polymer*, **30**, 509 (1989).
36. M. L. Williams, R. F. Landel, and J. D. Ferry, *J. Am. Chem. Soc.*, **77**, 3701 (1955).
37. J. D. Ferry, *Viscoelastic Properties of Polymers, 3rd Ed*, New York : Wiley (1980).
38. A. Killis, J. Le Nest, and H. Cheradame, *Makromol. Chem.*, **1**, 595 (1980).
39. H. Cheradame, in *IUPAC Macromolecules*; H. Benoit and P. Rempp, Eds.; Pergamon: London (1982).
40. H. Vogel, *Phys. Z.*, **22**, 645 (1921).
41. G. Tammann, W. Hesse, *Z. Anorg Allg.Chem.*, **156**, 245 (1926).
42. G. S. Fulcher, *J. Am. Ceram. Soc.*, **8**, 339 (1925).
43. M. Armand, *Solid State Ionics*, **9-10**, 745 (1983).
44. S. H. Kim, J. Y. Kim, H. S. Kim, and H. N. Cho, *Solid State Ionics*, **116**, 63 (1999).
45. C. A. Angell and R. D. Bressel, *J. Phys. Chem.*, **76**, 3244 (1972).
46. Harwood, L. M.; Moody, C. J. *Experimental Organic Chemistry*; Blackwell Scientific Publications: Oxford, 1989.
47. Jungk, S. J.; Gandour, R. D. *Organic Preparations and Procedures International*, **15**, 152 (1983).
48. Guo, C.; Chen, Q. *Huaxue Xuebao*, **42**, 592 (1984).
49. Huang, W.; Wang, W.; Huang, B. *Huaxue Xuebao*, **44**, 488 (1986).
50. Keck, G. E.; Yates, J. B. *J. Am. Chem. Soc.*, **104**, 5829 (1982).
51. Keck, G. E.; Enholm, E. J.; Yates, J. B.; Wiley, M. R. *Tetrahedron*, **41**, 4079 (1985).
52. Leibner, J. E.; Jacobus, J. *J. Org. Chem.*, **44**, 449 (1979).
53. Truce, W. E.; Vrencur, D. J. *J. Org. Chem.*, **35**, 1226 (1970).
54. Feuer, H.; Auerbach, M. *J. Org. Chem.*, **35**, 2551 (1970).
55. Chen, Q.; Zhu, R.; Li, Z.; Wang, S.; Huang, W. *Huaxue Xuebao*, **40**, 337 (1982).
56. Hansen, R. L.; *J. Org. Chem.*, **30**, 4322 (1965).
57. *CRC Handbook of Chemistry and Physics, 81st Edition*, Lide, D. R., Ed., CRC Press LLC: Boca Raton, 2000.
58. Subramanian, L. R.; Bentz, H.; Hanack, M. *Synthesis*, **5**, 293 (1973).
59. Volkov, N. D.; Nazaretyan, V. P.; Yagupol'skii, L. M. *Zhurnal Organicheskoi Khimii*, **18**, 519 (1982).
60. Subramanian, L. R.; Martinez, A. G.; Fernandez, A. H.; Alvarez, R. M. *Synthesis*, **6**, 481 (1984).

61. Marshall, D. B.; Strohbusch, F.; Eyring, E. M. *J. Phys. Chem.*, **85**, 2270 (1981).
62. Hojo, M.; Hasegawa, H.; Mizobe, A.; Ohkawa, Y.; Miimi, Y. *J. Phys. Chem.*, **99**, 16609 (1995).
63. Reyes, A.; Scott, R. M. *J. Phys. Chem.*, **84**, 3600 (1980).
64. Chen, M.-J.; Taylor, S. D. *Tet. Lett.*, **40**, 4149 (1999).
65. Kotoris, C. C.; Chen, M.-J.; Taylor, S. D. *J. Org. Chem.*, **63**, 8052 (1998).
66. Scott, W. J.; Crisp, G. T.; Stille, J. K. *J. Am. Chem. Soc.*, **106**, 4630 (1984).
67. Scott, W. J.; Stille, J. K. *J. Am. Chem. Soc.*, **108**, 3033 (1986).
68. Echavarren, A. M.; Stille, J. K. *J. Am. Chem. Soc.*, **109**, 5478 (1987).
69. *Personal Communication*, Customer Service, Aldrich Chemical Company.
70. Apfel, M. A.; Finkelmann, H.; Janini, G. M.; Laub, R. J.; Luhmann, B.-H.; Price, A.; Roberts, W. L.; Shaw, T. J.; Smithy, C. A. *Anal. Chem.*, **57**, 651 (1985).
71. Nestor, G.; White, M. S.; Gray, G. W.; Lacey, D.; Toyne, K. J. *Makromol. Chem.*, **188**, 2759 (1987).
72. Lewis, L. N.; Lewis, N. *Chem. Mater.*, **1**, 106 (1989).
73. Lewis, L. N.; *J. Am. Chem. Soc.*, **112**, 5998 (1990).
74. Lewis, L. N.; Lewis, N. *J. Am. Chem. Soc.*, **108**, 7228 (1986).
75. Lewis, L. N.; Uriarte, R. J. *Organometallics*, **9**, 621 (1990).
76. Speier, J. L. *Adv. Organomet. Chem.*, **17**, 407 (1979).
77. Lewis, L. N. *Chem.Rev.*, **93**, 2693 (1993).
78. The reference peak for TMS overlaps with the methyl peaks associated with polymethylsiloxane
79. Papke, B. L.; Ratner, M. A.; Shriver, D. F. *J. Phys. Chem. Solids*, **42**, 493 (1981).
80. Doan, K. E.; Heyen, B. J.; Ratner, M. A.; Shriver, D. F. *Chem. Mat.*, **2**, 539 (1990).